

The shape of dark matter halo in the PRG NGC 4262

Sergei Khoperskov,^{1,2} Alexei Moiseev,^{3,2} Alexander Khoperskov,⁴ and Anna Saburova²

¹*Institute of Astronomy, Russian Academy of Sciences, Pyatnitskaya st., 48, 119017 Moscow, Russia*

²*Sternberg Astronomical Institute, Moscow MV Lomonosov State University, Universitetskij pr., 13, 119992 Moscow, Russia*

³*Special Astrophysical Observatory, Russian Academy of Sciences, Nizhnii Arkhyz, Karachai-Cherkessian Republic, 357147, Russia*

⁴*Volgograd State University, Universitetsky pr., 100, 400062 Volgograd, Russia*

Abstract. With the aim to determine the spatial distribution of dark matter, we investigate the polar ring galaxy NGC 4262. We used the stellar kinematics data for the central galaxy obtained from optical spectroscopy together with information about the kinematics of the neutral hydrogen for polar component. It was shown that NGC 4262 is the classic polar ring galaxy case with the relative angle of 88° between components. From simulations of the central galaxy and ring kinematics we found that the shape of the dark matter distribution varies strongly with the radius. Namely, the dark matter halo is flattened towards the galactic disk plane $c/a = 0.4$, however it is prolate to the orthogonal (polar) plane far beyond the central galaxy $c/a = 1.7$. Also, the simulations of the ring evolution let us to confirm the stability of the ring and the formation of quasi-spiral structures within it.

1. Introduction

It was believed that galactic polar structures are the result of close interaction of galaxies, accretion of companion's matter or even cold gaseous filaments. In any case, polar ring galaxies (PRGs) appear to be a good probe to study the dark and baryonic matter gravitational potential around them. The general idea is that polar component should be stabilized by the dark matter (DM). Rotating in two perpendicular planes gives the opportunity to measure the spatial distribution of the gravitating matter in 3D due to the decomposition of rotation. Measurements of the kinematics and amount of the baryonic matter allowed us to constrain the mass and shape of the dark matter halo. Theoretical predictions pointed out that halo should be flattened towards the polar plane (Sparke 1986; Steiman-Cameron & Durisen 1982). Numerous investigations of the individual PRGs agree with that (e.g. Arnaboldi et al. 1993; Combes & Arnaboldi 1996; Iodice et al. 2003). However, the amount of real objects with the well-measured halo axis ratio is still limited. Based on new observations we decided to enlarge the sample of the known PRGs with measured shape parameters of the DM. In this paper we present new results, which are obtained for NGC 4262.

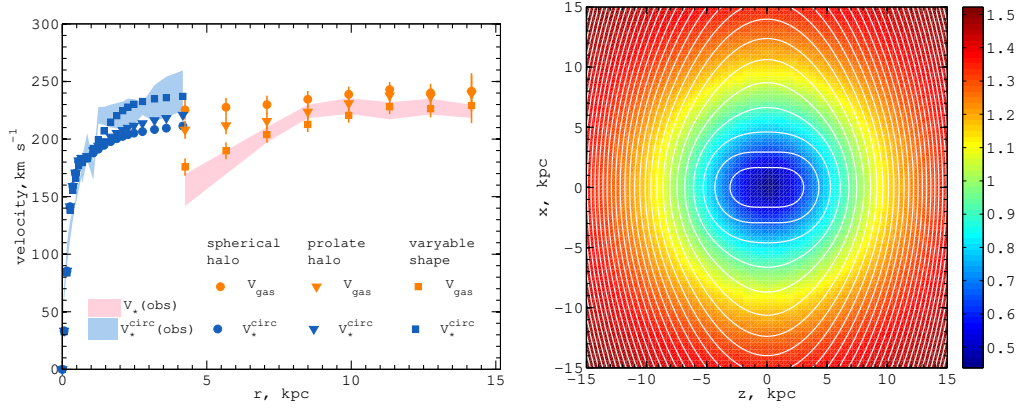


Figure 1. Left plot: observed kinematics of NGC 4262 (filled) and best-fit models for the spherical halo (circle), prolate halo (triangle) and variable shape halo (square). Right plot: contours of the halo potential for the best-fit model. Color represents the value of the halo axis ratio.

1.1. Observations

The central object is the early-type barred galaxy (Emsellem et al. 2004). The external wide HI ring beyond the stellar disk of the galaxy was discovered by Krumm et al. (1985). Bettoni et al. (2010) showed that a small contribution of stellar population observed in UV bands is presented in the ring, which is significantly inclined or even polar to the central disk (see also the comments in Buson et al. 2011). The galaxy seems to be an ideal object for our simulations because the polar ring mostly consists of the gaseous component with well-determined surface mass density distribution and kinematics. We used new 21-cm WSRT observations presented in Oosterloo et al. (2010) to calculate the gas density distribution and rotation curve of the ring as well. Elliptic beam was taken into account for the rotation curve reconstruction (see figure 1, left) with the help of the TiRiFiC software (Józsa et al. 2007). Rotation curve and velocity dispersion of the CG were derived from the long-slit observations with the multi-mode focal reducer SCORPIO-2 (Afanasiev & Moiseev 2011) at the SAO RAS 6-m BTA telescope. Analysis of kinematics and morphology properties of CG and PR gives us the mutual angle between the components $\delta = 50 \pm 6^\circ$ or $\delta = 88 \pm 6^\circ$. Thus, the second value corresponds to the classic polar ring galaxy case.

1.2. Halo model

Our kinematical models of both the CG and PR are based on the assumption of the stability of the ring. We simulated the line-of sight velocity field of the PR and circular velocity of the CG simultaneously. The circular velocity for CG (figure 1, left) was calculated from the asymmetric drift equation using the information about stellar velocity dispersion distribution along a radius. The isothermal halo density profile was used in the simulations. Three general types of the DM halo shape were tested: spherical halo, oblate halo and variable shape halo. Using χ^2 minimization we showed that the models with spherical and prolate halo do not reproduce well the observed kinematics of NGC 4262 (see figure 1). In these models the simulated circular velocity of the CG is systematically lower than observed. Vice versa gaseous rotation amplitude in the polar

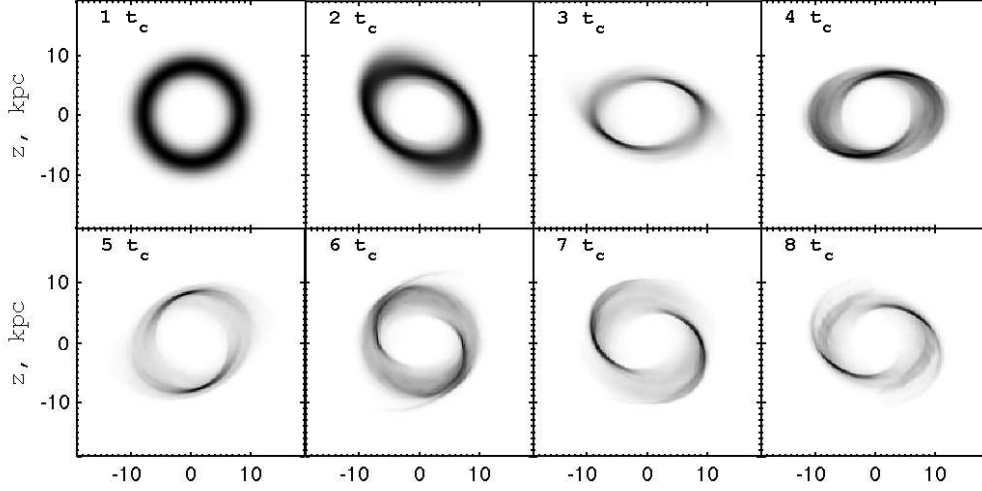


Figure 2. Time dependent evolution of the column density of the gaseous polar component.

plane is a bit higher than observed, especially in the inner region of the ring. Thus, to achieve the better agreement with observations we investigate the model with variable shape of DM potential. For the gravitational potential the following axis ratio model was accepted (Hayashi et al. 2007):

$$c/a = \exp [\alpha \tanh (\gamma \log (r/r_\alpha))], \quad (1)$$

where parameters α , γ and r_α determine the character of the halo shape. The best fit model implies the strong transformation of the halo axis ratio with radius. Better agreement between simulated and observed kinematics was found for $\alpha = 0.9 \pm 0.3$, $\gamma = 0.68 \pm 0.09$ and $r_\alpha = 1.33 \pm 0.2$. The result is clearly seen in the left panel of figure 1. The central part of the halo (within $r < 5$ kpc) is flattened towards the CG plane: $c/a = 0.4$. At $r \approx 5$ kpc it is round, and far beyond CG the halo is flattened towards the polar plane $c/a = 1.54$ at $r = 15$ kpc. In figure 1 (right) we show both the contours of the potential and c/a colormap. Smaller central value of the c/a gives low halo spatial scale leading to the faster increasing of the circular velocity of CG. At the same time high effective halo scale in the polar plane gives the slow growth of the rotation velocity for the polar component.

Despite the variable shape of DM around galaxies is expected from the different numerical simulations (e.g. Snaith et al. 2012), there is not much evidence of such halo type in galaxies. The first evidences of the variable halo shape were obtained for the Milky Way from the analysis of the stellar streams (Vera-Ciro & Helmi 2013). Flaring of the gas layer at the outskirts of the Galaxy also agrees with the non-constant halo axis ratio (Banerjee & Jog 2011). The question is whether the halo consists only of the collisionless matter or it includes also the dark baryonic gas. Unfortunately, within the current work there is no opportunity to separate dissipative and baryonic fraction of the NGC 4262 halo.

1.3. Dynamical simulations

Dynamical simulations are the important tool to test the stability of the polar component within the complicated gravitational potential obtained above. Our model is based on the hydrodynamical simulations of the evolution of the gaseous ring which is submerged into the massive dark matter halo. Simulations were performed using grid-based TVD MUSCL scheme. The initial conditions correspond to the best-fit model of the variable DM shape from previous paragraph. We neglected the contribution of the ring component to the total gravitational potential, because its total stellar and gaseous masses were low. Figure 2 shows the time dependent evolution of the column density of the gas in the polar plane. The polar ring is stable during numerous periods of rotation. However, the non-axisymmetric perturbation from the halo generates the spiral structure in the gaseous polar ring. The influence of the DM shape is larger than the perturbation from the disk at the distances of 5 – 15 kpc from the center. Global spiral pattern could lead to the formation of the dense regions where the star formation processes should be driven. These morphological features are the similar to the arc-like (or spiral fragment) structure with the ongoing star formation in the northern-west side of the polar ring of NGC 4262 detected on the *GALEX* UV images (Bettoni et al. 2010).

Acknowledgments. This work was supported by the RFBR grants 12-02-00685, 12-02-31452, 13-02-00416 and the “Active Processes in Galactic and Extragalactic Objects” basic research program of the Department Physical Sciences of the RAS OFN-17. S.K., A.M. and A.S. are also grateful for the financial support of the ‘Dynasty’ Foundation. The observations at the 6-m telescope were carried out with the financial support of the Ministry of Education and Science of Russian Federation (contracts no. 16.518.11.7073 and 14.518.11.7070).

References

- Afanasiev, V. L., & Moiseev, A. V. 2011, *Baltic Astronomy*, 20, 363
- Arnaboldi, M., Capaccioli, M., Cappellaro, E., Held, E. V., & Sparke, L. 1993, *A&A*, 267, 21
- Banerjee, A., & Jog, C. J. 2011, *ApJ*, 732, L8. 1103. 5821
- Bettoni, D., Buson, L. M., & Galletta, G. 2010, *A&A*, 519, A72
- Buson, L. M., Bettoni, D., & Galletta, G. 2011, *Ap&SS*, 335, 231
- Combes, F., & Arnaboldi, M. 1996, *A&A*, 305, 763
- Emsellem, E., Cappellari, M., Peletier, R. F., McDermid, R. M., Bacon, R., Bureau, M., Copin, Y., Davies, R. L., Krajnović, D., Kuntschner, H., Miller, B. W., & de Zeeuw, P. T. 2004, *MNRAS*, 352, 721
- Hayashi, E., Navarro, J. F., & Springel, V. 2007, *MNRAS*, 377, 50
- Iodice, E., Arnaboldi, M., Bournaud, F., Combes, F., Sparke, L. S., van Driel, W., & Capaccioli, M. 2003, *ApJ*, 585, 730
- Józsa, G. I. G., Kenn, F., Klein, U., & Oosterloo, T. A. 2007, *A&A*, 468, 731
- Krumm, N., van Driel, W., & van Woerden, H. 1985, *A&A*, 144, 202
- Oosterloo, T., Morganti, R., Crocker, A., Jütte, E., Cappellari, M., de Zeeuw, T., Krajnović, D., McDermid, R., Kuntschner, H., Sarzi, M., & Weijmans, A.-M. 2010, *MNRAS*, 409, 500
- Snaith, O. N., Gibson, B. K., Brook, C. B., Knebe, A., Thacker, R. J., Quinn, T. R., Governato, F., & Tissera, P. B. 2012, *MNRAS*, 425, 1967
- Sparke, L. S. 1986, *MNRAS*, 219, 657
- Steiman-Cameron, T. Y., & Durisen, R. H. 1982, *ApJ*, 263, L51
- Vera-Ciro, C., & Helmi, A. 2013, *ApJ*, 773, L4